Oligomeric Hsp33 with Enhanced Chaperone Activity

GEL FILTRATION, CROSS-LINKING, AND SMALL ANGLE X-RAY SCATTERING (SAXS) ANALYSIS*

Mohd. Waseem Akhtar‡, Volety Srinivas‡, Bakthisaran Raman‡, Tangirala Ramakrishna‡, Tomonao Inobe§, Kosuke Maki§, Munehito Arai¶, Kunihiro Kuwajima§, and Ch. Mohan Rao‡∥

From the ‡Centre for Cellular and Molecular Biology, Hyderabad 500 007, India, the §Department of Physics, School of Science, University of Tokyo and CREST Japan Science and Technology Agency, 7-3-1 Hongo Bunkyo-ku, Tokyo 113-0033, Japan, and the ¶Protein Design Research Group, Institute for Biological Resources and Functions, National Institute of Advanced Industrial Science and Technology (AIST), Tsukuba Central 6, 1-1-1 Higashi, Tsukuba, Ibaraki 305-8566, Japan

Hsp33, an *Escherichia coli* cytosolic chaperone, is inactive under normal conditions but becomes active upon oxidative stress. It was previously shown to dimerize upon activation in a concentration- and temperature-dependent manner. This dimer was thought to bind to aggregation-prone target proteins, preventing their aggregation. In the present study, we report small angle x-ray scattering (SAXS), steady state and time-resolved fluorescence, gel filtration, and glutaraldehyde cross-linking analysis of full-length Hsp33. Our circular dichroism and fluorescence results show that there are significant structural changes in oxidized Hsp33 at different temperatures. SAXS, gel filtration, and glutaraldehyde cross-linking results indicate, in addition to the dimers, the presence of oligomeric species. Oxidation in the presence of physiological salt concentration leads to significant increases in the oligomer population. Our results further show that under conditions that mimic the crowded milieu of the cytosol, oxidized Hsp33 exists predominantly as an oligomeric species. Interestingly, chaperone activity studies show that the oligomeric species is much more efficient compared with the dimers in preventing aggregation of target proteins. Taken together, these results indicate that in the cell, Hsp33 undergoes conformational and quaternary structural changes leading to the formation of oligomeric species in response to oxidative stress. Oligomeric Hsp33 thus might be physiologically relevant under oxidative stress.

Oxidative stress generated by the production of reactive oxygen species is an inevitable consequence of aerobic life. In addition, the extracellular environment can also cause oxidative stress to the cells (1, 2). Heat shock is shown to increase oxidative stress (3). Oxidative stress, *inter alia*, results in misfolding and aggregation of several cellular proteins. In order to combat oxidative stress, cells produce proteins that detoxify reactive oxygen species and repair harmful changes. The *Escherichia coli* cytoplasm, like that of most other organisms, is largely reducing in nature although under oxidative stress, the redox status of the cell changes significantly. Several cellular proteins are regulated by redox-dependent post-translational modifications (4).

Until recently, no molecular chaperone was known that could be turned on or off by a post-translational event acting as a switch. Jakob *et al.* (5) showed that a member of the highly conserved cytoplasmic prokaryotic molecular chaperones, Hsp33, is regulated by the redox state of the medium. Under reducing conditions, Hsp33 is inactive. Hsp33 has four absolutely conserved cysteine residues: Cys-232, -234, -265, and -268. In the reduced state, they are coordinated to a zinc atom (6). Oxidizing conditions lead to the release of zinc and formation of two intramolecular disulfide bonds, Cys-232 with Cys-234 and Cys-265 with Cys-268 (7). Upon such oxidative activation, Hsp33 binds to aggregation-prone states of proteins, preventing their aggregation and acting as a holdase chaperone (5, 7, 8). We have earlier shown that there are significant secondary and tertiary structural differences between the reduced and oxidized forms of Hsp33. Our studies showed that conformational changes accompanied by increased exposure of hydrophobic surfaces, are involved in the oxidative activation of Hsp33 (9).

Initial studies by Jakob *et al.* (5), based on gel filtration and cross-linking data, suggested that Hsp33 might act as a monomer (5). Subsequently, the crystal structure of Hsp33 was reported by two groups (10, 11). Interestingly, both studies showed that Hsp33 existed in a domain-swapped dimeric form. One of the studies suggested that the increase in concentration of Hsp33, brought about under conditions of heat stress, favors dimerization (12). It is important to note that the reported crystal structure lacks about 60 residues in the C terminus.

In the present study, we have used small angle x-ray scattering (SAXS),[1] fluorescence, gel filtration, and glutaraldehyde cross-linking analysis of full-length Hsp33 to investigate structural and conformational changes in Hsp33 upon oxidation at different temperatures. Our results show that upon oxidative stress there are significant structural and conformational changes in oxidized Hsp33 at different temperatures, leading to the formation of higher oligomeric species, ranging from dimer to octamer. Chaperone activity studies show that the oligomeric species is much more efficient compared with the dimer. Taken together, our results suggest that in the cell, Hsp33 exists predominantly as an oligomeric species upon oxidative stress.

∥ To whom correspondence should be addressed: Center for Cellular and Molecular Biology Hyderabad 500 007, India. Tel.: 91-40-2719-2543; Fax: 91-40-2716-0591; E-mail: mohan@ccmb.res.in; Web: www.ccmb.res.in/staff/mohan.

[1] The abbreviations used are: SAXS, small angle x-ray scattering; PEG, polyethylene glycol; DTT, dithiothreitol; IPTG, isopropyl-1-thio-β-D-galactopyranoside; BSA, bovine serum albumin; bis-ANS, 1,1′-bis(4-anilino)naphthalene-5,5′-disulfonic acid; CS, citrate synthase; FPLC, fast protein liquid chromatography.

MATERIALS AND METHODS

1,1′-Bis(4-anilino)naphthalene-5,5′-disulfonic acid (Bis-ANS), citrate synthase (from porcine heart), dithiothreitol (DTT), glutaraldehyde, PEG 3350, and PEG 8000 were purchased from Sigma. Sephadex G-75, Superdex G-75, Superose 6, Superose 12 HR 10/30 FPLC columns, and phenyl-Sepharose CL 6B fast flow were obtained from Amersham Biosciences. Isopropyl-1-thio-β-D-galactopyranoside (IPTG) was obtained from Bangalore Genei, Bangalore, India and acrylamide (3×) was from Sisco Research Laboratory, Mumbai, India. H_2O_2 and other chemicals used in this study were of analytical reagent grade.

Overexpression and Purification of Hsp33—*E. coli* Hsp33 was cloned as described earlier (9). Competent *E. coli* BL21 (DE3) cells were transformed with the expression plasmid pET21a-Hsp33. Primary culture was grown overnight from transformed cells at 37 °C, and 1% inoculum of this primary culture was added to 1 liter of medium containing 100 μg/ml ampicillin for the secondary culture at 37 °C and 250 rpm. The secondary culture was grown until $OD_{600\ nm}$ of the culture reached 0.6–0.8. The culture was then induced with 1 mM IPTG and grown for 5 more hours. Along with IPTG, $ZnSO_4$ was added to a final concentration of 1 mM. After induction, the cells were harvested by centrifugation at 6,000 rpm for 10 min. The harvested cells were stored at −20 °C.

The cells were resuspended (3 ml of buffer per gram of pellet) in 50 mM Tris-HCl buffer (pH 7.4) containing 100 mM NaCl, 1 mM EDTA (TEN buffer), and 10 μM phenylmethylsulfonyl fluoride was added. Cells were lysed by sonication, and the cell debris was removed by centrifugation at 14,000 rpm for 20 min at 4 °C. The cell lysate was subjected to ammonium sulfate fractionation. Hsp33 precipitated between 15 and 50% saturation by ammonium sulfate. The precipitate was dissolved in TEN buffer and the protein solution applied to a Sephadex G-75 column (150 cm × 1.8 cm diameter) equilibrated with TEN buffer and was eluted at a flow rate of 20 ml/h using the same buffer with a fraction size of 2 ml. Fractions containing Hsp33 were pooled, and 200 mM ammonium sulfate was added to the protein. This protein solution was applied to a phenyl-Sepharose column previously equilibrated with 50 mM potassium phosphate buffer (pH 7.0) containing 200 mM ammonium sulfate. The column was developed using 50 mM potassium phosphate buffer (pH 7.0). Fractions containing pure Hsp33 were pooled, concentrated, and buffer exchanged with buffer A (40 mM HEPES-KOH, pH 7.5, containing 20 mM KCl and 200 μM of $ZnSO_4$) using Amicon ultrafiltration unit and stored at −70 °C.

Preparation of Reduced and Oxidized Hsp33—For chaperone assays, small angle x-ray scattering studies, and other experiments, purified Hsp33 was oxidized with 10 mM H_2O_2 for 4 h at different temperatures. Reduced Hsp33 was prepared by incubating the purified Hsp33 with 10 mM DTT for 2 h. For gel filtration studies, Hsp33 was reduced with 5 mM β-mercaptoethanol for 2 h at 25 °C and subsequently oxidized by 10 mM H_2O_2 for varying durations at different temperatures.

Gel Filtration Studies—Oligomer formation was studied by gel filtration chromatography using a Superdex G-75 or Superose-12 HR 10/30 FPLC column. 80 μl of Hsp33 (1 mg/ml) oxidized in the presence or the absence of 500 mM NaCl was loaded on the Superdex G-75 column equilibrated with 50 mM Tris-HCl, pH 7.4, with or without 500 mM NaCl, respectively. To study the effect of NaCl concentration, Hsp33 oxidized at 43 °C in the presence of various concentrations of NaCl was loaded on a Superose-12 column previously equilibrated with the Tris-HCl buffer containing the appropriate concentration of NaCl. Molecular mass standards comprising blue dextran (2,000 kDa), BSA (67 kDa), ovalbumin (45 kDa), and RNase A (13.7 kDa) were used for calibration. Oligomer sizes, in the presence of PEG, were determined using Superose-6 HR 10/30 FPLC column. Hsp33 oxidized at 43 °C in the presence of 100 mg/ml PEG and 100 mM NaCl was applied to the column equilibrated with 50 mM Tris-HCl, pH 7.4 and eluted at a flow rate of 0.3 ml/min. High molecular mass standards comprising BSA (67 kDa), catalase (232 kDa), and thyroglobulin (669 kDa) were used for calibration.

SDS-PAGE—Glutaraldehyde cross-linking studies on reduced Hsp33 or Hsp33 oxidized at 43 °C in the presence of 150 or 500 mM NaCl for 4 h were performed with 0.05, 0.1, 0.2, and 0.5% glutaraldehyde for 2 h at 25 °C. The cross-linked products were loaded onto a 7.5% SDS-polyacrylamide gel and visualized by silver staining.

To investigate the involvement of intermolecular disulfide bonds in the formation of higher oligomers, samples of reduced Hsp33 or Hsp33 oxidized at 43 °C in the presence of 500 mM NaCl or 100 mg/ml PEG 8000 for 4 h were loaded on a 12% non-reducing SDS-polyacrylamide gel, and bands were visualized by Coomassie Blue R-250 staining.

Small Angle X-ray Scattering Studies—The SAXS experiments were performed at beamline 15A of the Photon Factory at the High Energy Accelerator Research Organization, Tsukuba, Japan (13). The experimental details and the analysis of the scattering data were essentially the same as described earlier (14). The sample solution in 1-mm path length mica-windowed cell was exposed to a monochromatic x-ray beam (1.5 Å). The temperature of the sample solution was maintained at 25 °C using a circulating water bath. Scattering patterns were recorded by a CCD-based x-ray detector, which consisted of a beryllium-windowed x-ray image intensifier (Be-XRII) (Hamamatsu, V5445P-MOD), an optical lens, a CCD image sensor, and a data acquisition system (Hamamatsu C7300) (14, 15). The camera length was set to be 1485 or 2375 mm depending on the scattering-angle region to be observed.

The R_g and I (0) values were obtained using the Guinier approximation. $\ln I(Q) = \ln I(0) − (Q^2 R_g{}^2)/3$, at small angle regions where $\ln I(Q)$ is linearly dependent on Q^2. Q and I (Q) are the momentum transfer and intensity at zero scattering angle, respectively. Q is defined as $Q = 4\pi \sin\theta/\lambda$, where 2θ is the scattering angle, and λ is the wavelength of the X-rays, 1.5 Å (16, 17). The theoretical R_g values of Hsp33 monomer and dimer were calculated from the crystal structure (11) using the program Crysol (18). To obtain shape information, the scattering data were converted to $P(r)$ function by GNOM software using a D_{max} value of 71 Å (19). The $P(r)$ function was taken to DAMMIN to generate *ab initio* shape data (20). This process was repeated 11 times and then averaged using DAMAVER. The high resolution, crystal structure data of Hsp33 (PDB 1HW7), and the *ab initio* shape data obtained from DAMMIN program were matched using SUPCOMB (21).

Chaperone Assays—Citrate synthase is known to undergo aggregation upon heating at temperatures above 40 °C (22). Citrate synthase (0.02 or 0.025 mg/ml) in 40 mM HEPES-KOH, pH 7.5, was incubated at 43 °C. Light scattering was monitored in a Hitachi F-4000 fluorescence spectrophotometer equipped with a thermostatted cell holder and stirrer. The measurements were performed by setting the excitation and emission wavelengths at 360 nm and the excitation and emission band passes at 3 nm. To study the effect of NaCl, Hsp33 oxidized in the presence of 150 or 500 mM NaCl was used in the assay. Similarly, to study the effect of PEG, Hsp33 oxidized in buffer containing 100 mg/ml PEG 8000 and 100 mM NaCl was used in the assay. Aggregation of citrate synthase in the presence of required concentrations of NaCl or PEG alone were used as controls. Percent protection of aggregation was calculated relative to these controls. Percent protection of aggregation was calculated as $(I_{cs} − I_{cs+Hsp33})/I_t × 100$, where I_t is the intensity of scattered light for citrate synthase alone at the end of the assay, and $I_{cs+Hsp33}$ is the intensity of light scattered by the citrate synthase in the presence of Hsp33.

Fluorescence Measurements—All fluorescence spectra were recorded using a Hitachi F-4010 fluorescence spectrophotometer. Intrinsic protein fluorescence of reduced and oxidized Hsp33 (0.2 mg/ml) was recorded by exciting the sample at 285 nm. The emission spectra were recorded from 295 to 380 nm by setting the excitation and emission slit widths at 5 nm and 3 nm, respectively. Time-resolved fluorescence quenching measurements were performed with the neutral quencher, acrylamide, using a picosecond time-correlated photon counting setup described earlier (23). A Ti-sapphire femto/picosecond laser (Spectra Physics, Mountain View, CA) pumped by an Nd:YLF Laser (Millenia X, Spectra Physics) was used. 1-ps pulses of 888 nm radiation from the Ti-sapphire laser were frequency tripled to 295 nm using a frequency doubler/tripler (GWU, Spectra Physics). Fluorescence decay curves were obtained using a time-correlated single photon counting setup, coupled to a microchannel plate photomultiplier (model 2809u; Hamamatsu Corporation). The instrument response function (IRF) was obtained at 295 nm using a dilute colloidal suspension of bright nondairy coffee whitener. The half-width of IRF was ~40 ps. The samples were excited at 295 nm, and the fluorescence emission was collected through a 310-nm cutoff filter followed by a monochromator at 340–350 nm. The cutoff filter was used to prevent the scattering of the excitation beam from the samples. In fluorescence lifetime measurements, the emission was measured at the magic angle (54.7°) to eliminate the contribution from the decay of anisotropy. The fluorescence decay curves at the magic angle were analyzed by deconvoluting the observed decay with IRF to obtain the intensity decay function represented as a sum of three exponentials: $I(t) = \Sigma \alpha_i \exp(−t/\tau_i)$ i = 1 − 3, where $I(t)$ is the fluorescence intensity at time t and α_i is the amplitude of the ith lifetime τ_i, such that $\Sigma_i \alpha_i = 1$.

Tryptophan time-resolved fluorescence intensity measurements for reduced Hsp33 and Hsp33 oxidized at 25, 37, and 43 °C were made in the absence and the presence of various concentrations of acrylamide in buffer A. The concentration of Hsp33 used was 0.33 mg/ml.

To probe the hydrophobic surfaces of the protein, polarity-sensitive fluorescent probe bis-ANS was used (24). Stock solution of bis-ANS was
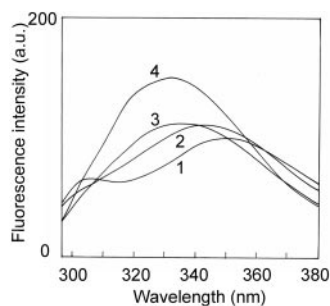
FIG. 1. **Intrinsic fluorescence emission spectra of reduced Hsp33 (*curve 1*) and Hsp33 oxidized at 25 °C (*curve 2*), 37 °C (*curve 3*), and 43 °C (*curve 4*) respectively.** The concentration of Hsp33 was 0.2 mg/ml. The excitation wavelength was 285 nm. Excitation and emission band passes were set at 5 and 3 nm, respectively.

prepared in methanol. To 0.2 mg/ml reduced or oxidized Hsp33 in buffer A, bis-ANS was added to a final concentration of 5 μM. Fluorescence spectra of the samples were recorded from 400 to 600 nm with the excitation wavelength set at 390 nm. Excitation and emission band passes were set at 5 nm. All spectra were recorded in the corrected spectrum mode.

RESULTS AND DISCUSSION

Temperature-dependent Structural Changes in Hsp33— Hsp33 is inactive as a chaperone in its reduced form, and oxidation is known to activate it to prevent the aggregation of target proteins. It provides an interesting example of a post-translational event acting as a switch to regulate the chaperone-like activity of Hsps. We have shown earlier that oxidative activation is associated with conformational change and increase in hydrophobicity (9). Many small heat shock proteins are known to undergo temperature-dependent changes in their structure, which modulates their chaperone activity. We have previously shown that α-crystallin undergoes structural alteration above 30 °C, resulting in the re-organization of its hydrophobic surfaces and a concomitant increase in its chaperone activity (25–27). The small heat shock protein, Hsp22 also exhibits temperature-dependent changes in the tertiary structure and increase in chaperone activity (28). Earlier studies have shown increase in chaperone activity of Hsp33 as a function of temperature; at elevated temperatures, the rate of Hsp33 dimerization is higher suggesting the involvement of structural rearrangements (12). We have investigated, using fluorescence and CD spectroscopy, the structural changes of Hsp33 as a function of temperature. Fig. 1 shows the intrinsic fluorescence spectra of reduced Hsp33 and Hsp33 oxidized at 25, 37, and 43 °C. Reduced Hsp33, upon exciting at 285 nm, exhibits an emission maximum at 351 nm whereas Hsp33 oxidized at 25 °C shows emission maximum at 346 nm. When Hsp33 is oxidized at elevated temperatures (37 and 43 °C), it shows larger blue shifts in the tryptophan emission maximum, the maxima being 335 and 330 nm at 37 °C and 43 °C, respectively. It is evident from Fig. 1 that the lone tryptophan residue of reduced Hsp33 is exposed to the solvent; oxidation leads to its burial in the hydrophobic environment. This process is much more pronounced at elevated temperatures, indicating conformational and/or quaternary structural changes. Reduced Hsp33 shows a less intense emission maximum, in addition to 351-nm emission, at around 305 nm (Fig. 1). This fluorescence (305 nm) is quenched upon oxidation. This result is in conformity with that of Graumann *et al.* (12) who observed quenched tyrosine fluorescence accompanied by substantially broadened fluorescence spectra suggesting an increased energy transfer between tyrosine and tryptophan residues.

In order to investigate the accessibility of the lone tryptophan, we have carried out tryptophan lifetime measurements
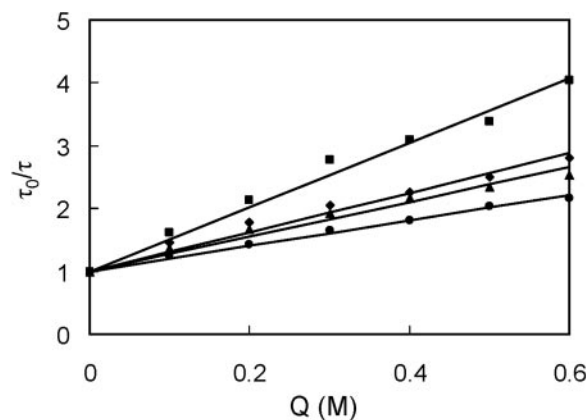

FIG. 2. **Stern-Volmer plot of acrylamide quenching of tryptophan lifetime fluorescence.** Reduced Hsp33 at 25 °C (*filled squares*), Hsp33 oxidized at 25 °C (*filled diamonds*), 37 °C (*filled triangles*), and 43 °C (*filled circles*) are shown. τ_0 and τ are the fluorescence lifetimes before and after the addition of acrylamide. Q is the molar acrylamide concentration. The concentration of Hsp33 was 0.33 mg/ml.

of reduced Hsp33 and Hsp33 oxidized at 25, 37, and 43 °C in the absence and presence of acrylamide. Fig. 2 shows the effect of increasing acrylamide concentration on the ratio of τ_0/τ (where τ_0 represents the lifetime in the absence of quencher, and τ is the lifetime in the presence of various concentrations of quencher) in reduced Hsp33 and Hsp33 oxidized at 25, 37, and 43 °C. Our time-resolved fluorescence data show that oxidation leads to increased burial of the lone tryptophan residue of Hsp33. The slopes of these plots yield the Stern-Volmer constants (K_{sv}), and the ratio of K_{sv} and τ yields the bimolecular quenching constant, K_q. Table I shows the average lifetimes, K_{sv} values, and the bimolecular quenching constants of Hsp33 under reduced and oxidized conditions. Upon oxidation, we have observed a slight increase in the average lifetime of the lone tryptophan residue and a 3-fold decrease in the bimolecular quenching constants (Table I). These results show that Hsp33 undergoes structural changes upon oxidation; the lone tryptophan residue, which is exposed in reduced Hsp33, gets buried in a relatively more hydrophobic environment upon oxidation at elevated temperatures.

Near-UV CD spectra of Hsp33 oxidized at 25 and 43 °C show distinct differences in the 255–290 nm region, suggesting altered conformation upon oxidation at elevated temperatures (data not shown). Taken together, fluorescence and CD spectroscopy data clearly indicate that Hsp33 undergoes temperature-dependent conformational change upon oxidation.

*Oligomerization of Hsp33—*Initial studies by Jakob *et al.* (5) suggested that Hsp33 is monomeric even upon activation, but subsequent biochemical and crystal structure studies on Hsp33 suggested that it forms dimers (10, 11). The dimerization of oxidized Hsp33 as well as chaperone-like activity is temperature-dependent (12). However, glutaraldehyde cross-linking of the truncated Hsp33 (residues 1–235) in the presence of the target protein, luciferase, suggested the possibility of the formation of higher oligomers (10). We have investigated in detail the process of oligomerization upon oxidation of Hsp33. We have used gel filtration (Superdex G-75) to investigate the temperature-dependent dimerization of Hsp33. Fig. 3 shows the effect of temperature on the dimerization of Hsp33. *Panel I* in Fig. 3*A* shows the chromatogram of reduced Hsp33, whereas *panel II* shows that of Hsp33 oxidized at 25 °C. As can be seen from these panels, oxidation at 25 °C does not lead to dimerization, even after 4 h of oxidation (*panel III*). At 37 °C, reduced Hsp33 is monomeric (Fig. 3*B*, *panel I*), upon oxidation for 30 min, 1, 2, and 4 h, the dimer population gradually increases (*panels II-V*).

TABLE I
Lifetimes and quenching parameters obtained from time-resolved fluorescence studies

	Lifetime[a]		K_{sv}	Bimolecular quenching constant K_q
	τ_0	τ_{600}		
	ns		M^{-1}	$M^{-1}\,s^{-1}$
Red Hsp33	2.5	0.62	5.13	2.05×10^9
Ox Hsp33				
25 °C	2.8	1	3.13	1.12×10^9
37 °C	3	1.19	2.77	0.92×10^9
43 °C	2.9	1.32	2.02	0.69×10^9

[a] τ_0 and τ_{600} are the average lifetimes obtained in the absence and in the presence of 600 mM acrylamide, respectively.

The population of the dimer increases significantly at the heat shock temperature, 43 °C, with much reduced content of monomer (Fig. 3*C*, *panel II-V*). Interestingly, at later time points, a small population of oligomeric species could also be seen. This result indicates that Hsp33 could form oligomeric species upon oxidation at physiological (37 °C) and heat shock temperatures (43 °C), which might have functional significance. At all the temperatures studied, reduced Hsp33 remained monomeric (*panel I* of Fig. 3, *A–C*).

Since hydrophobic interactions are enhanced in the presence of salt, we studied the effect of NaCl on the quaternary structure of Hsp33 upon oxidation as a function of temperature. Fig. 4*A* (*panel II*) shows that Hsp33 oxidized at 25 °C remains largely monomeric with a small extent of dimerization even in the presence of salt. Hsp33 oxidized at 37 °C, was a mixture of monomer, dimer, and higher order species that eluted in the void volume of the Superdex G-75 column (Fig. 4*B*). However, Hsp33 oxidized at 43 °C, eluted almost completely in the void volume on a Superdex G-75 column, with a small amount of monomer and dimer (Fig. 4*C*). These results suggest that Hsp33 oxidized at elevated temperatures in the presence of 500 mM NaCl undergoes oligomerization and that the oligomerization is driven by hydrophobic interactions. Because the oligomers eluted in the void volume, the oligomers should be more than 75 kDa.

Considering that the oligomeric species elute in the void volume of the Superdex G-75 column, we have carried out gel filtration studies using Superose 12 column, which can better resolve the higher oligomeric species. Fig. 5 shows gel filtration profiles of reduced Hsp33 and Hsp33 oxidized in presence of increasing concentrations of NaCl. Reduced Hsp33 elutes from the column as a monomer. Addition of physiologically relevant salt concentration (150 mM NaCl) results in the formation of predominant amounts of dimeric species in addition to some amounts of higher oligomers. The elution profile of Hsp33 oxidized in the presence of higher salt concentrations (300 and 500 mM NaCl) exhibits a hump corresponding to a tetramer (~130 kDa) and even larger aggregates that appear toward the void volume of the column, which correspond to an octamer (~300 kDa), the exclusion limit of Superose 12. This suggests that addition of salt strengthens oligomer formation, which is polydisperse in nature.

In order to further confirm the oligomerization status of Hsp33, we performed glutaraldehyde cross-linking of Hsp33 oxidized at 43 °C in the presence of 150 and 500 mM NaCl. When cross-linked in the presence of 0.05% glutaraldehyde, Hsp33 oxidized at 43 °C in the presence of 150 mM NaCl exhibits bands corresponding to monomer, dimer, and a very small proportion of higher oligomers, which appears to be at least more than hexamer (Fig. 6, *lane 1*). Oligomers, as seen in SDS-PAGE, increase as the concentration of glutaraldehyde is increased from 0.05 to 0.5% (Fig. 6, *lanes 1–4*). On the other hand, in the case of reduced Hsp33, no cross-linked products

were observed even when the maximum concentration of glutaraldehyde (0.5%) was used (Fig. 6, *lane 6*) showing that reduced Hsp33 exists exclusively as monomer. A similar cross-linking experiment was also performed in the presence of 500 mM NaCl (Fig. 6, *lanes 8–10*). In conformity with our earlier gel filtration data, we observed an increased proportion of dimer and higher oligomers in the presence of 0.05% glutaraldehyde, and as the concentration of glutaraldehyde is increased, larger proportions of dimer, tetramer, and higher oligomers are seen (Fig. 6, *lanes 8–10*).

Oligomeric state appears to be important for chaperone-like activity of heat shock proteins. Small angle x-ray scattering is an excellent tool to investigate the sizes and shapes of biomolecules in solution, which is important for understanding their physiological roles. We have investigated the scattering profile of reduced Hsp33 and Hsp33 oxidized in the presence and absence of added salt. Fig. 7 shows a Guinier plot for reduced Hsp33. Non-linear least-squares curve fitting of the data to ln $I(Q) = \ln I(0) - (Q^2 R_g^2)/3$ (see "Materials and Methods") yield R_g value of 22.40 Å. This R_g value, for reduced Hsp33, is in excellent agreement with the expected value of 22.54 Å for the Hsp33 monomer calculated using the crystal structure (PDB 1HW7).

The reported crystal structure of Hsp33 lacks about 60 residues toward the C terminus (10, 11). The structural information available on the truncated Hsp33 does not explain why reduced Hsp33 has no chaperone activity. Our SAXS data are from full-length Hsp33. Despite this, the R_g value estimated from crystal structure and that of the full-length Hsp33 obtained from SAXS measurements are in excellent agreement. This suggests that either the reduced form of full-length Hsp33 is more compact or the additional C-terminal region can fold onto the molecule without increasing the R_g value. In order to explore these possibilities, we have carried out *ab initio* low resolution shape calculation as described by Svergun (20). The low resolution shape data are matched with high resolution structure data using a procedure described by Kozin and Svergun (21). Fig. 8 shows the superposition of the two matched structures. The SAXS envelop fits the crystal structure; interestingly, however, the SAXS *ab initio* profile has unoccupied regions and exhibits some difference from the crystal structure. The differences indicate a possibility of minor conformational changes between the truncated crystal structure and the full-length protein investigated in SAXS experiments. It is possible that the unoccupied region might accommodate the remaining 60 residues of the full-length protein, making it a compact structure without any significant change in the R_g value. Thus, reduced Hsp33 may exist as a monomer with the C terminus folding over the remaining structure, perhaps masking the target protein binding site, resulting in the lack of chaperone activity. Graf *et al.* (29) showed that the C-terminal zinc binding domain is fully folded in the reduced zinc-coordinated state, which masks the dimerization interface and the substrate binding site. Upon oxidation the C-terminal domain of Hsp33 unfolds, dramatically exposing the substrate binding site and unmasking the dimerization interface. Our results are in agreement with the observations of Graf *et al.* (29).

The simulated scattering profile from the crystal structure, the Q *versus* $I(Q)$ plot, of Hsp33 fits well with the measured scatter profile (Fig. 9*A*). A similar profile, simulated using a dimeric structure (from crystal structure coordinates) deviates from the scatter profile of the oxidized Hsp33 obtained from SAXS measurements (Fig. 9*B*). This observation indicates that the molecular species in the solution of oxidized Hsp33 may contain dimers and oligomers. Such profile measured from the sample oxidized in the presence of 500 mM NaCl deviates mark-
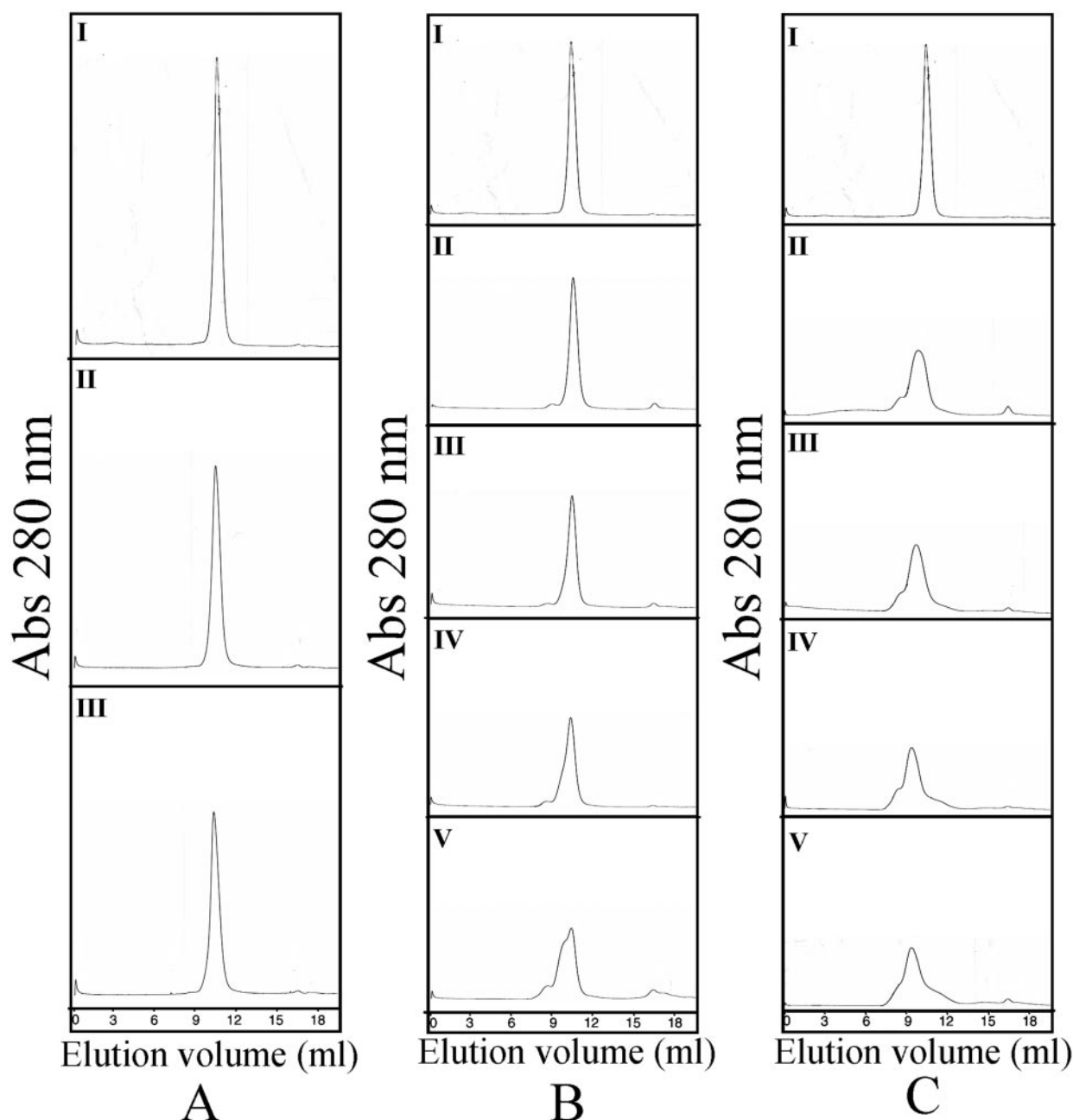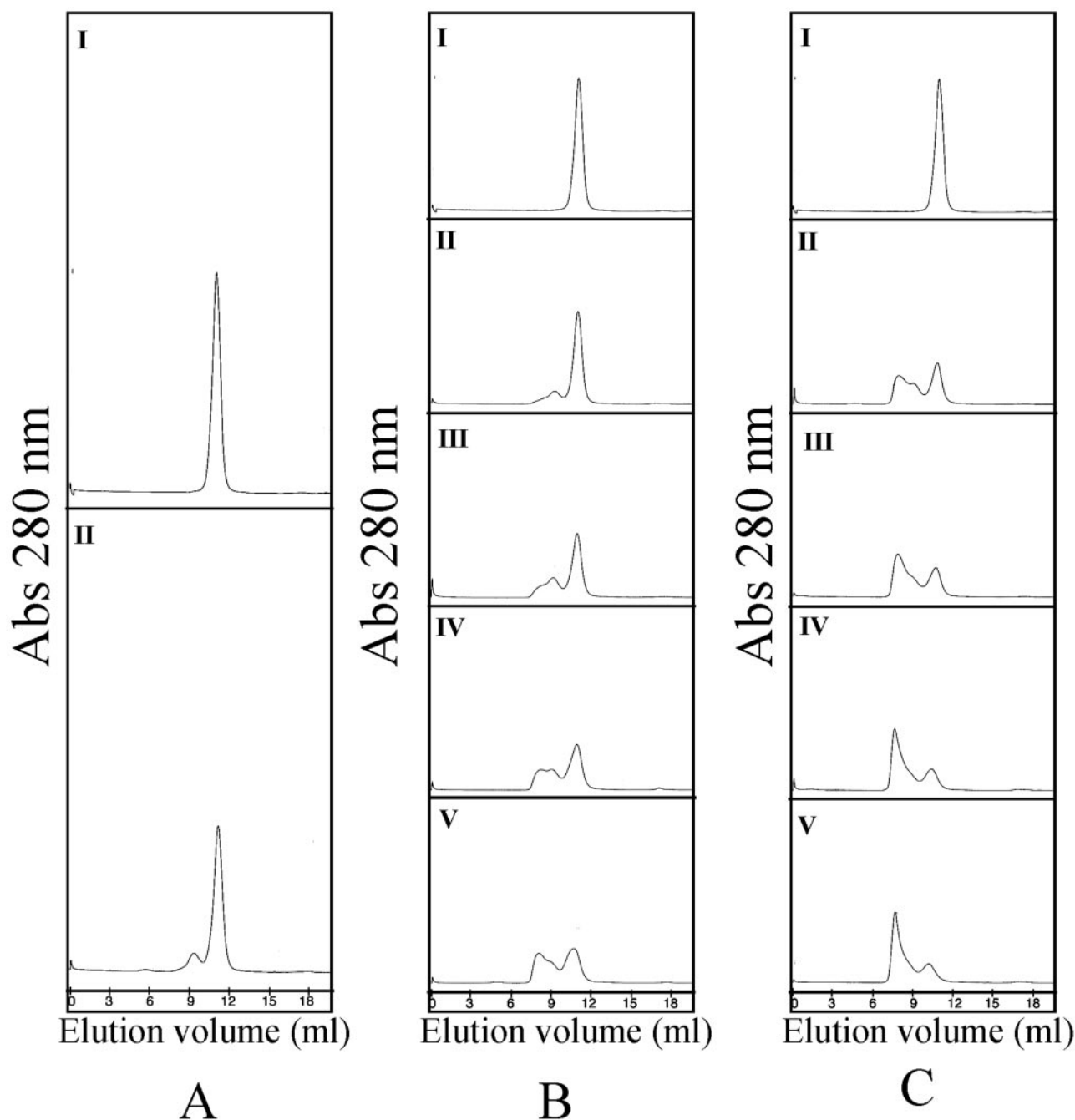
FIG. 3. **Gel filtration studies of Hsp33 upon oxidation at various temperatures as a function of time in the absence of NaCl.** Reduced Hsp33 or Hsp33 oxidized at the required temperature, dissolved in 40 mM HEPES buffer, pH 7.5, containing 20 mM KCl, was loaded on a Superdex G-75 FPLC column. Reduced Hsp33 was oxidized at 25 °C (*A*), 37 °C (*B*), or at 43 °C (*C*). In *A, panel I* depicts the gel filtration pattern of reduced Hsp33, while *panels II* and *III* depict the profiles after 2 and 4 h of oxidation at 25 °C. In *B* and *C, panel I* depicts reduced Hsp33, whereas *panels II, III, IV,* and *V* depict the profiles 30 min, 1, 2, and 4 h after oxidation at 37 and 43 °C respectively.

edly from the simulated profile (Fig. 9*C*), consistent with the predominant presence of oligomers.

The R_g value obtained from SAXS measurements for oxidized Hsp33 is more than 35 Å, in contrast to the theoretical (dimeric) value of 24.1 Å. The molecular mass of the oxidized Hsp33, as measured from SAXS data, is around 85 kDa, which is different from the expected molecular mass of the dimeric Hsp33 (66 kDa) suggesting that apart from a major dimer component, Hsp33 tends to form oligomeric (larger than dimeric) species under oxidizing conditions. This is in concurrence with our gel filtration data. Hsp33 upon oxidation, in the presence of 200 mM NaCl, shows an R_g value of around 50 Å and molecular mass of about 200 kDa. These values suggest that under salt conditions oxidized Hsp33 forms higher oligomers. This result is in agreement with our gel filtration as

well as glutaraldehyde cross-linking data. Thus, SAXS measurements appear to reveal some valuable structural information on the molecular status of Hsp33 in solution.

Inside the cell, the concentration of macromolecules is so high that a significant proportion of the volume is physically occupied and, therefore, unavailable to other molecules. Because of this excluded volume effect, the effective concentration of each macromolecule increases significantly (30, 31). Crowding agents such as polyethylene glycol, ficoll, and dextran mimic the crowded cellular environment and increase the effective concentration of the protein (32). We investigated whether Hsp33 could oligomerize in the presence of the crowding agent PEG, which mimics physiologically relevant conditions *in vitro*. Fig. 10 shows gel filtration chromatographs of reduced Hsp33, and Hsp33 oxidized in the presence of PEG

FIG. 4. **Gel filtration studies of Hsp33 upon oxidation at various temperatures as a function of time in the presence of NaCl.** Reduced Hsp33 or Hsp33 oxidized at the required temperature, dissolved in 40 mM HEPES buffer, pH 7.5, containing 20 mM KCl and 500 mM NaCl, was loaded on a Superdex G-75 FPLC column. Reduced Hsp33 was oxidized at 25 °C (*A*), 37 °C (*B*), or at 43 °C (*C*). In *A*, *panel I* depicts the gel filtration pattern of reduced Hsp33, whereas *panel II* depicts the profile after 4 h of oxidation. In *B* and *C*, *panel I* depicts reduced Hsp33, whereas *panels II*, *III*, *IV*, and *V* depict the profiles 30 min, 1, 2, and 4 h after oxidation at 37 and 43 °C, respectively.

3350 and PEG 8000. As can be seen from the figure, both PEG 3350 and PEG 8000 induce oligomerization of oxidized Hsp33, the extent of oligomerization is more in the presence of PEG 8000 compared with that in the presence of PEG 3350.

In order to verify whether the formation of higher order species is caused by formation of intermolecular disulfide bonds we have performed non-reducing SDS-PAGE of Hsp33 under different conditions. As expected, reduced Hsp33 yielded a single band corresponding to ~33 kDa in the absence of any added reagents (Fig. 11, *lane 1*) or in the presence of 500 mM NaCl (Fig. 11, *lane 2*) or 100 mg/ml of the crowding agent PEG (Fig. 11, *lane 3*). The increased mobility of reduced Hsp33 in the presence of 100 mg/ml PEG (Fig. 11, *lane 3*) may be caused by

compaction of the molecule. Hsp33 oxidized at 43 °C in the absence of any added reagents also showed a single band corresponding to ~33 kDa. In the presence of 500 mM salt, Hsp33 oxidized at 43 °C also shows a band at 33 kDa. In addition to this, a very faint band is seen at ~97 kDa; this band represents a very small fraction of the total protein, suggesting that the higher order species are held together largely by hydrophobic interactions. The absence of such higher molecular mass bands in the presence of 100 mg/ml PEG indicate that in the presence of the crowding agent, the formation of higher order species is entirely caused by hydrophobic interactions.

Hydrophobic interactions between the chaperones and target proteins are known to play an important role in the binding of
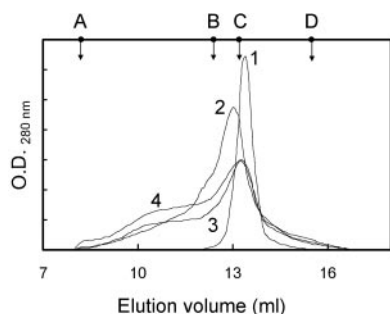
Oligomeric Hsp33 with Enhanced Chaperone Activity

FIG. 5. **Gel filtration studies of Hsp33 oxidized at 43 °C as a function of NaCl concentration.** Reduced Hsp33 (*curve 1*) or Hsp33 oxidized at 43 °C in 40 mM HEPES buffer, pH 7.5, containing 150 mM (*curve 2*), 300 mM (*curve 3*), or 500 mM NaCl (*curve 4*) was loaded on a Superose-12 FPLC column. *Solid circles* with *arrows* indicate the elution positions of molecular mass standards (*A*, blue dextran; *B*, BSA; *C*, ovalbumin, and *D*, RNase A).
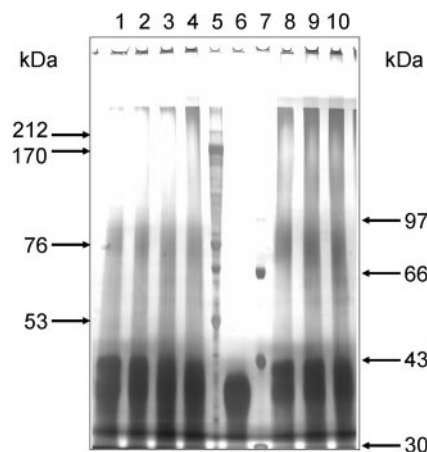
FIG. 6. **Glutaraldehyde cross-linking of reduced and oxidized Hsp33.** Hsp33 (0.33 mg/ml) was oxidized at 43 °C for 4 h in the presence of 150 or 500 mM NaCl. Glutaraldehyde was added to a final concentration of 0.05% (*lanes 1* and *8*), 0.1% (*lanes 2* and *9*), 0.2% (*lanes 3* and *10*), and 0.5% (*lanes 4* and *6*). The protein samples were incubated for 2 h at room temperature in the presence of glutaraldehyde. *Lanes 1–4*, Hsp33 oxidized in the presence of 150 mM NaCl; *lane 5*, high molecular mass markers; *lane 6*, reduced Hsp33; *lane 7*, low molecular mass markers, and *lanes 8–10*, Hsp33 oxidized in the presence of 500 mM NaCl.
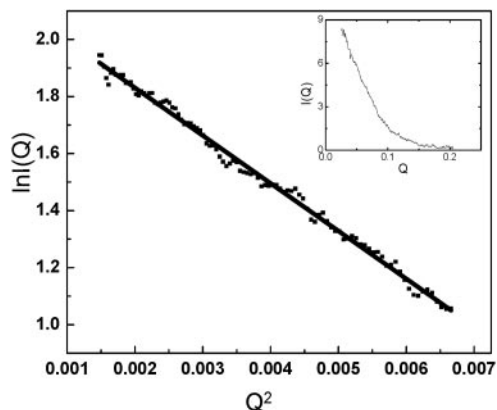

FIG. 7. **Guinier plot of reduced Hsp33 obtained from the scattering curve in the small angle region.** The concentration of Hsp33 was 2.8 mg/ml. Hsp33 was dissolved in 40 mM HEPES buffer (pH 7.5) containing 20 mM KCl and 10 mM DTT. *Inset*, scattering profile of reduced Hsp33 in the entire scattering region starting from the beamstop.

chaperones to the non-native states of target proteins and prevention of aggregation. We have used bis-ANS to probe the hydrophobic surface of Hsp33, in its reduced form and upon oxida-
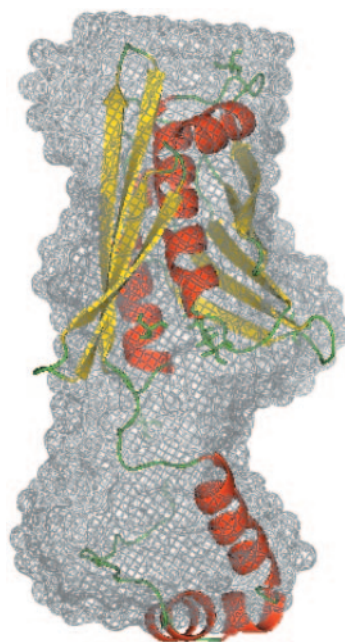

FIG. 8. **Superimposition of reduced Hsp33 *ab initio* shape with crystal structure.** *Ab initio* shape was generated from SAXS data using DAMMIN program (11 independent iterations were performed and averaged with DAMAVER). The resultant DAMAVER file was superimposed with monomeric Hsp33 crystal structure using SUPCOMB.

tion at 43 °C in the presence and absence of 500 mM NaCl. Reminiscent of our earlier data (9), Hsp33 in the reduced form shows very little bis-ANS binding at 43 °C. Upon oxidation in the absence of NaCl, there is significant increase in bis-ANS binding (9). As can be seen from Fig. 12, there is a 2-fold increase in bis-ANS binding when the oxidation of Hsp33 is carried out in the presence of 500 mM NaCl at 43 °C compared with that in the absence of salt. As mentioned above, Hsp33 oxidized in the absence of NaCl exists predominantly as a dimer, whereas when oxidized in the presence of 500 mM NaCl, it is predominantly oligomeric in nature. Our result thus shows that Hsp33 exhibits increased hydrophobic surfaces in the oligomer compared with the dimer as monitored by bis-ANS binding.

Enhanced Chaperone Activity of Hsp33 Oligomer—In order to investigate whether the oligomeric species is functionally active, we have studied the chaperone activity of Hsp33 oxidized under conditions that populate largely either the monomer, the dimer, or the oligomer. We have used the thermally induced aggregation of citrate synthase as the model system to monitor the chaperone-like activity. Fig. 13*A* shows the results of such an experiment. DTT or H_2O_2, at the concentrations used for reducing or oxidizing Hsp33, did not affect the aggregation of citrate synthase in control experiments (data not shown). Reduced Hsp33 did not prevent the aggregation of citrate synthase even when added in a 5-fold molar excess over the target protein as reported earlier (5). Hsp33 oxidized at 25 °C also did not prevent aggregation of CS at a chaperone to CS molar ratio of 0.3:1; it postponed the process by a few minutes. However, at a higher molar ratio it prevented the aggregation of CS (data not shown). Under these conditions, Hsp33 is predominantly in a monomeric state (See Fig. 3*A*). On the other hand, Hsp33 oxidized at 43 °C exhibited ~57% prevention of aggregation at a molar ratio of 0.3:1. Under these conditions Hsp33 exists predominantly as dimer (Fig. 3*C*). Hsp33 oxidized at 43 °C in the presence of 150 mM NaCl prevented the aggregation to an extent of ~85%. Hsp33 oxidized at 43 °C in the presence of 500 mM NaCl prevented the aggrega-
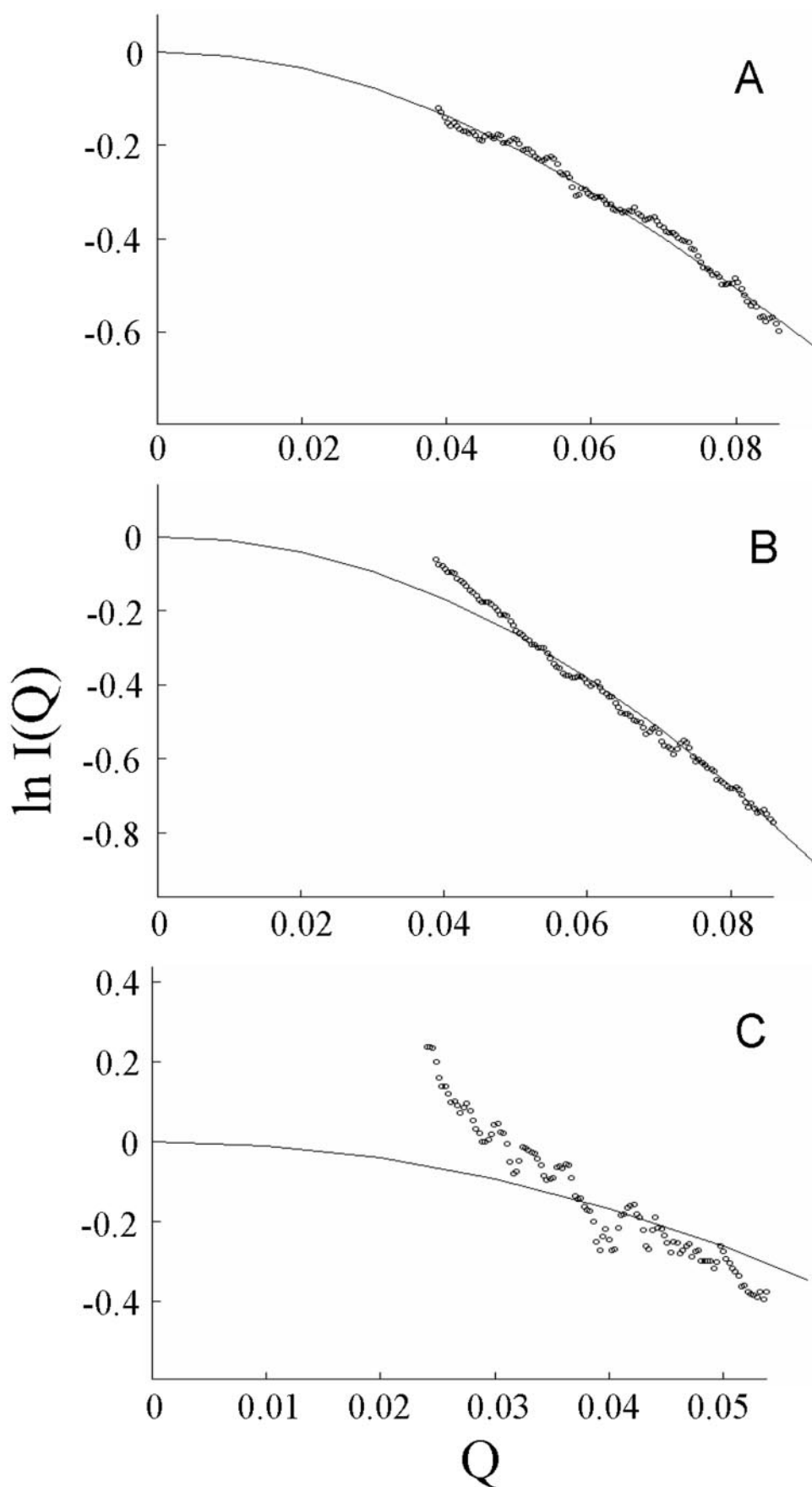
FIG. 9. **Guinier plots of Hsp33 obtained with SAXS measurements fitted with crystal structure data using the CRYSOL program.** *A*, plot of reduced Hsp33 fitted with monomer crystal coordinates (PDB 1HW7). *B*, plot of oxidized Hsp33 fitted with dimer crystal structure coordinates. *C*, plot of Hsp33 oxidized in the presence of 200 mM NaCl fitted with dimer crystal structure coordinates.
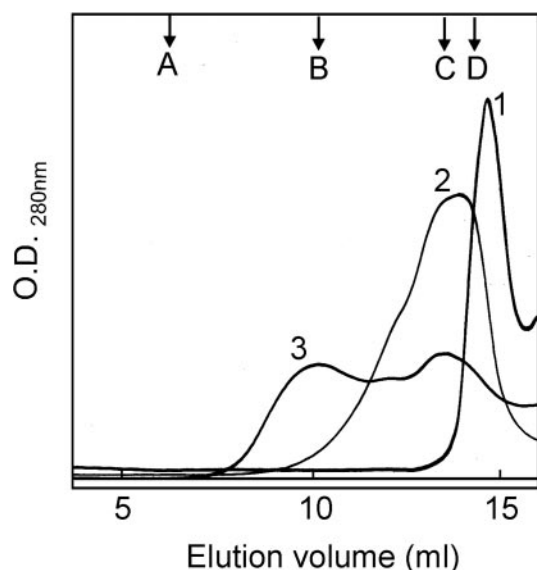
Oligomeric Hsp33 with Enhanced Chaperone Activity

FIG. 10. **Gel filtration chromatography of reduced Hsp33 in PEG 8000 (*curve 1*) and Hsp33 oxidized at 43 °C in the presence of PEG 3350 (*curve 2*) or PEG 8000 (*curve 3*).** *Arrows* indicate the elution positions of molecular mass standards (*A*, blue dextran; *B*, thyroglobulin; *C*, catalase, and *D*, BSA).
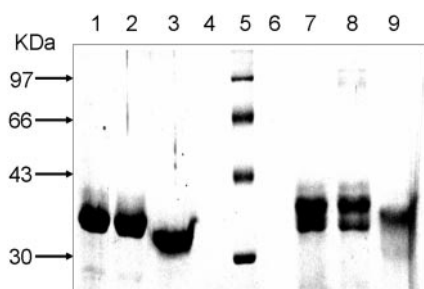

FIG. 11. **Non-reducing SDS-PAGE of reduced and oxidized Hsp33.** *Lane 1*, reduced Hsp33; *lane 2*, reduced Hsp33 in the presence of 500 mM NaCl; *lane 3*, reduced Hsp33 in the presence of 100 mg/ml PEG 8000; *lane 5*, molecular mass markers; *lane 7*, oxidized Hsp33; *lane 8*, Hsp33 oxidized in the presence of 500 mM NaCl; *lane 9*, Hsp33 oxidized in the presence of 100 mg/ml PEG 8000.
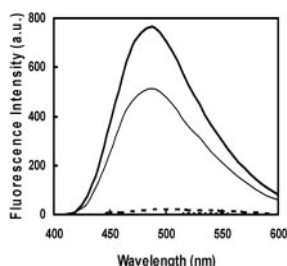

FIG. 12. **Bis-ANS binding to reduced and oxidized Hsp33 in the presence and absence of 500 mM NaCl.** Oxidation of Hsp33 was carried out at 43 °C, and the fluorescence measurements were done at 25 °C. The excitation and emission bandwidths were set at 5 nm, and the protein solution containing bis-ANS was excited at 390 nm. The fluorescence emission spectra represented are as follows: bis-ANS bound to reduced Hsp33, *thick dashed line*; Hsp33 oxidized in the presence of 500 mM NaCl, *thick solid line*; and Hsp33 oxidized in the absence of NaCl, *thin solid line*. Bis-ANS blank spectrum is represented by a *thin dashed line*.

FIG. 13. **Chaperone activity of Hsp33 toward the heat-induced aggregation of CS under various conditions.** *A*, CS (0.02 mg/ml) in 40 mM HEPES-KOH, pH 7.5, was incubated at 43 °C in the absence (*curve 1*) or the presence of Hsp33 oxidized at 25 °C (*curve 2*), 43 °C (*curve 3*), 43 °C with 150 mM NaCl (*curve 4*), or 43 °C with 500 mM NaCl (*curve 5*). All the reactions had the same final NaCl concentration in the chaperone activity assay. A chaperone to target protein molar ratio of 0.3:1 was used. *B*, CS (0.025 mg/ml) in 40 mM HEPES-KOH, pH 7.5, was incubated at 43 °C in the absence (*curve 1*) or the presence of Hsp33 oxidized at 43 °C (*curve 2*) or 43 °C with 100 mM NaCl and 100 mg/ml PEG 8000 (*curve 3*). All the reactions had the same final NaCl and PEG 8000 concentrations in the chaperone activity assay. A chaperone to target protein molar ratio of 0.2:1 was used.

activity compared with the Hsp33 dimer formed in the absence of crowding agent (Fig. 13*B*), Hsp33 dimer offers ~14% protection, whereas oligomeric Hsp33 offers ~82% protection against thermally induced aggregation of citrate synthase.

Thus, our results show that oxidized Hsp33 can form large oligomers either in the presence of NaCl or in the presence of crowding agents such as PEG; the oligomeric species exhibits significantly higher chaperone activity compared with the oxidized dimeric Hsp33. Enhancement of chaperone activity upon oligomer formation has previously been reported in the case of other chaperones. Hsp90 normally occurs as a dimer. Studies by Yonehara *et al.* (33) showed that heating induces the chaperone activity of Hsp90, which is latent under normal conditions. They further showed that only the higher oligomers formed upon heating possess chaperone activity and not the native dimers. Rogalla *et al.* (34) demonstrated that large oligomers of Hsp27 are necessary for chaperone activity and resistance against oxidative stress. Upon phosphorylation, Hsp27 dissociates into tetramers and loses these activities.

Very recently, Graf *et al.* (29) have shown that the N-terminal region of Hsp33 does not undergo any significant change upon oxidation; on the other hand, the C-terminal region harboring the zinc binding motif, which adopts a predominantly helical conformation in the reduced, zinc-bound Hsp33, undergoes significant unfolding with concomitant zinc release and disulfide bond formation. This unfolding results in the loss of helicity and renders the C-terminal domain highly unstructured. The lone tryptophan of Hsp33 present toward the C-terminal shows blue-shifted fluorescence as oxidation temperature is increased suggesting that there is differential unfolding at different temperatures. The results obtained in the present study using SAXS, gel filtration, and glutaralde-

tion to an extent of ~98%. Under these conditions, Hsp33 exists as a polydisperse oligomer (Fig. 5). These results clearly demonstrate that whereas monomers are inactive, dimers are active, but the oligomers are significantly more active than the dimers. Interestingly, the oligomer of Hsp33 formed in the presence of PEG 8000 also shows significantly more chaperone
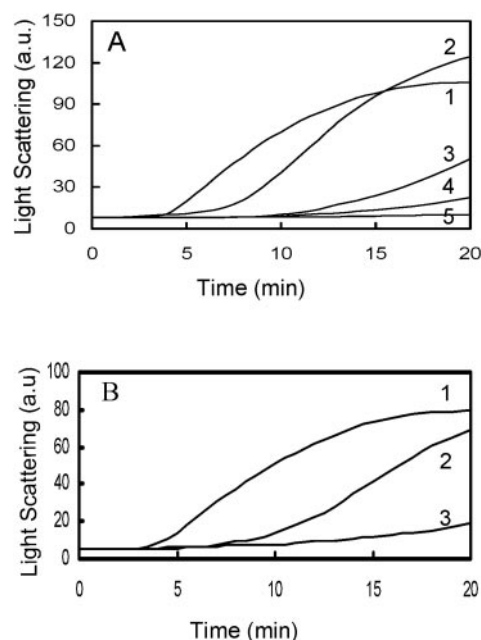
hyde cross-linking clearly demonstrate that Hsp33, when oxidized at elevated temperatures in the presence of physiologically relevant concentrations of salt or crowding agents such as polyethylene glycol, forms higher order oligomers. We speculate that the C-terminal domain facilitates higher order oligomerization of Hsp33, because this domain is unstructured and flexible in solution. Increased oligomer formation in the presence of high salt concentrations suggests that oligomer formation is largely driven by hydrophobic interactions; nonreducing SDS-PAGE indicates that the involvement of intermolecular disulfide bonds appears to be minimal in this process. The fact that these oligomers of Hsp33 show higher chaperone activity compared with dimeric Hsp33 indicates that possibly Hsp33 in the cellular milieu exists as an oligomer rather than a dimer.

REFERENCES

1. Storz, G., and Imlay, J. A. (1999) *Curr. Opin. Microbiol.* **2,** 188–194
2. Imlay, J. A. (2003) *Annu. Rev. Microbiol.* **57,** 395–418
3. Davidson, J. F., Whyte, B., Bissinger, P. H., and Schiestl, R. H. (1996) *Proc. Natl. Acad. Sci. U. S. A.* **93,** 5116–5121
4. Paget, M. S., and Buttner, M. J. (2003) *Annu. Rev. Genet.* **37,** 91–121
5. Jakob, U., Muse, W., Eser, M., and Bardwell, J. C. (1999) *Cell* **96,** 341–352
6. Jakob, U., Eser, M., and Bardwell, J. C. (2000) *J. Biol. Chem.* **275,** 38302–38310
7. Barbirz, S., Jakob, U., and Glocker, M. O. (2000) *J. Biol. Chem.* **275,** 18759–18766
8. Hoffmann, J. H., Linke, K., Graf, P. C., Lilie, H., and Jakob, U. (2004) *EMBO J.* **23,** 160–168
9. Raman, B., Kumar, L. V. S., Ramakrishna, T., and Rao, C. M. (2001) *FEBS Lett.* **489,** 19–24
10. Kim, S. J., Jeong, D. G., Chi, S. W., Lee, J. S., and Ryu, S. E. (2001) *Nat. Struct. Biol.* **8,** 459–466
11. Vijayalakshmi, J., Mukhergee, M. K., Graumann, J., Jakob, U., and Saper, M. A. (2001) *Structure* (*Camb.*) **9,** 367–375
12. Graumann, J., Lilie, H., Tang, X., Tucker, K. A., Hoffmann, J. H., Vijayalakshmi, J., Saper, M., Bardwell, J. C., and Jakob, U. (2001) *Structure* (*Camb.*) **9,** 377–387
13. Amemiya, Y., Wakabayashi, K., Hamanaka, T., Wakabayashi, T., Matsushima, T., and Hashizume, H. (1983) *Nuclear Instrum. Methods* **208,** 471–477
14. Arai, M., Ito, K., Inobe, T., Nakao, M., Maki, K., Kamagata, K., Kihara, H., Amemiya, Y., and Kuwajima, K. (2002) *J. Mol. Biol.* **321,** 121–132
15. Amemiya, Y., Ito, K., Yagi, N., Asano, Y., Wakabayashi, K., Ueki, T., and Endo, T. (1995) *Rev. Sci. Instrum.* **66,** 2290–2294
16. Porod, G. (1982) in *Small Angle X-ray Scattering* (Glatter, O., and Kratky, O., eds) pp. 17–51, Academic Press, London
17. Kataoka, M., Nishii, I., Fujisawa, T., Ueki, T., Tokunaga, F., and Goto, Y. (1995) *J. Mol. Biol.* **249,** 215–228
18. Svergun, D. I., Barberato, C., and Koch, M. H. J. (1995) *J. Appl. Crystallogr.* **28,** 768–773
19. Svergun, D. I. (1992) *J. Appl. Crystallogr.* **25,** 495–503
20. Svergun, D. I. (1999) *Biophys. J.* **76,** 2879–2886
21. Kozin, M. B., and Svergun, D. I. (2001) *J. Applied Crystallogr.* **34,** 33–41
22. Jakob, U., Lilie, H., Meyer, I., and Buchner, J. (1995) *J. Biol. Chem.* **270,** 7288–7294
23. Lakshmikanth, G. S., and Krishnamoorthy, G. (1999) *Biophys. J.* **77,** 1100–1106
24. Musci, G., Metz, G. D., Tsunematsu, H., and Berliner, L. J. (1985) *Biochemistry* **24,** 2034–2049
25. Raman, B., and Rao, C. M. (1997) *J. Biol. Chem.* **272,** 23559–23564
26. Rao, C. M., Raman, B., Ramakrishna, T., Rajaraman, K., Ghosh, D., Datta, S., Trivedi, V. D., and Sukhaswami, M. B. (1998) *Int. J. Biol. Macromol.* **22,** 271–281
27. Rao, C. M., Ramakrishna, T., and Raman, B. (2002) *Proc. Ind. Natl. Sci. Acad.* **68,** 349–365
28. Chowdary, T. K., Raman, B., Ramakrishna, T., and Rao, C. M. (2004) *Biochem. J.* **381,** 379–387
29. Graf, P. C., Martinez-Yamout, M., VanHaerents, S., Lilie, H., Dyson, J. H., and Jakob, U. (2004) *J. Biol. Chem.* **279,** 20529–20538
30. Ellis, R. J. (2001) *Curr. Opin. Struct. Biol.* **11,** 114–119
31. Minton, A. P. (2000) *Curr. Opin. Struct. Biol.* **10,** 34–39
32. Martin, J., and Hartl, F. U. (1997) *Proc. Natl. Acad. Sci. U. S. A.* **94,** 1107–1112
33. Yonehara, M., Minami, Y., Kawata, Y., Nagai, J., and Yahara, I. (1996) *J. Biol. Chem.* **271,** 2641–2645
34. Rogalla, T., Ehrnsperger, M., Preville, X., Kotlyarov, A., Lutsch, G., Ducasse, C., Paul, C., Wieske, M., Arrigo, A. P., Buchner, J., and Gaestel, M. (1999) *J. Biol. Chem.* **274,** 18947–18956